Joaquim M. Gonçalves
joaquimm@ifsc.edu.br
Federal Institute of Santa Catarina
Air Conditioning and Refrigeration Center
88103310 São José, SC, Brazil

Cláudio Melo
melo@polo.ufsc.br
Federal University of Santa Catarina
Department of Mechanical Engineering
88040900 Florianópolis, SC, Brazil

Christian J. L. Hermes
chermes@ufpr.br
Federal University of Paraná
Department of Mechanical Engineering
81531990 Curitiba, PR, Brazil

Jader R. Barbosa, Jr.
jrb@polo.ufsc.br
Federal University of Santa Catarina
Department of Mechanical Engineering
88040900 Florianópolis, SC, Brazil

Experimental Mapping of the Thermodynamic Losses in Vapor Compression Refrigeration Systems

The present study introduces a methodology for mapping the thermodynamic losses of vapor compression refrigeration systems which consists of a theoretical model that splits the coefficient of performance into four terms: (i) the coefficient of performance of an ideal cycle (Carnot), (ii) the efficiency of a real cycle running with an ideal compressor, (iii) the compression efficiency of a real compressor, and (iv) the cycling efficiency. In addition, measurements of the relevant variables at several positions along the refrigeration loop are also required, generating performance data not only for the whole unit but also for each one of the system components. The proposed methodology points out the thermodynamic losses of the refrigeration system, identifying opportunities for energy performance improvement. In addition, the methodology is suitable for comparing different refrigeration systems with respect to the same thermodynamic baseline. Albeit the methodology was originally developed for household refrigerators, it can be easily extended to any kind of vapor-compression refrigeration systems.
Keywords: *vapor compression refrigeration, experimental analysis, thermodynamic losses, energy consumption*

Introduction

The performance of a household refrigerator is usually assessed by testing it in a controlled climatized chamber according to standardized test procedures that require the measurement of the overall power consumption over time as well as the temperatures at several locations along the refrigeration loop and within the refrigerated cabinet. In some particular cases, the suction and discharge pressures are also monitored to provide the condensing and evaporating temperatures, which are used for calculating the evaporator superheating and condenser subcooling. Although the standardized test procedures (e.g., AHAM HRF-1, 2004; ISO 15502, 2005) provide a broad amount of information, only a small part is actually utilized during the standardized data regression, which is aimed mainly at calculating the overall energy consumption for a certain set of operating conditions (surrounding and cabinet air temperatures). This information, however, is extremely limited when compared to what could be obtained if a thermodynamic mapping methodology was additionally employed.

Although alternative data processing approaches have been introduced in the literature (Bansal, 2003; Hermes et al., 2004) there is not a generalized methodology that is able to: (i) map the thermodynamic losses that take place in vapor compression refrigeration systems; (ii) compare the efficiency of a refrigeration system, after introducing a component-level modification to the efficiency of the previous configuration; and (iii) compare the efficiencies of different systems using the same thermodynamic baseline. The main focus of the present study is, therefore, to put forward a methodology that matches all these characteristics.

Basically, the methodology consists of splitting the coefficient of performance into four terms: (i) coefficient of performance of an ideal cycle (Carnot), (ii) efficiency of a real cycle operating with an ideal compressor, (iii) compression efficiency of the real compressor, and (iv) cycling efficiency, i.e., the thermodynamic losses due to the on-off control pattern. Measurements of the relevant variables at several positions along the refrigeration loop are also required, generating performance data not only for the whole unit, but also for each one of the cycle components. The tests were carried out with a typical 450-liter 'Combi' top-mount refrigerator designed for the North American market. The methodology is applicable to the refrigerator cycling regime, which represents the major part of experimental tests performed during the product development process. Although the methodology was developed for a household refrigerator, it can be easily extended to any kind of vapor compression refrigeration system spanning from residential to industrial refrigerating applications.

Paper accepted January, 2011. Technical Editor: José A. dos Reis Parise

Nomenclature

A	= *area,* m^2
COP	= *coefficient of performance, dimensionless*
h	= *specific enthalpy, J/kg*
N	= *compressor speed, Hz*
p	= *pressure, bar*
p_c	= *condensing pressure, bar*
p_e	= *evaporating pressure, bar*
Q	= *cooling capacity, W*
T	= *temperature, K*
T_{amb}	= *average temperature of the surrounding air, K*
T_{ff}	= *average fresh-food compartment temperature, K*
T_{fz}	= *average freezer compartment temperature, K*
T_{int}	= *average temperature of the cabinet air, K*
t_{off}	= *compressor off-cycle period, s*
t_{on}	= *compressor runtime, s*
UA_{ff}	= *fresh-food compartment conductance, W/K*
UA_{fz}	= *freezer compartment conductance, W/K*
v	= *specific volume,* m^3/kg
V	= *volume of the compression chamber,* m^3
w	= *refrigerant mass flow rate, kg/s*
W	= *power, W*
W_{actual}	= *power consumed by the real compressor, W*
W_{int}	= *power dissipation inside the cabinet, W*
W_s	= *power consumed by an ideal compressor, W*
W_{system}	= *power consumed by the whole system, W*

Greek Symbols

η = *thermodynamic efficiency, dimensionless*
η_g = *compressor overall efficiency, dimensionless*
η_v = *compressor volumetric efficiency, dimensionless*
ΔT = *temperature difference, K*

Subscripts

1 = *compressor suction*
2 = *compressor discharge, condenser inlet*
3 = *condenser outlet*
4 = *evaporator inlet*
5 = *evaporator outlet*
amb = *surrounding air*
actual = *refrigeration cycle with a real compressor*
c = *condenser*
cycle = *real cycle with an ideal (isentropic) compressor*
cycling = *cycling transients*
e = *evaporator*
ff = *fresh-food compartment*
fz = *freezer compartment*
ideal = *ideal (Carnot) cycle*
int = *cabinet air*
k = *compressor*
other = *other components (fans, heaters, lightning)*
s = *isentropic process*
system = *refrigeration system as a whole*

Thermodynamic Mapping

Power consumption of an ideal cycle (Carnot)

The power consumed by an ideal refrigeration cycle, where all the thermodynamic processes are reversible, is obtained from:

$$W_{ideal} = \frac{Q}{COP_{ideal}} \tag{1}$$

where Q is the cooling capacity [W], and the coefficient of performance of an ideal cycle, COP_{ideal}, is calculated from:

$$COP_{ideal} = \frac{T_{int}}{T_{amb} - T_{int}} \tag{2}$$

where T_{amb} is the ambient air temperature [K], and T_{int} is the average cabinet air temperature [K]. In cases where the refrigerator has two or more refrigerated compartments, the temperature T_{int} is calculated as follows. Firstly, the compartment thermal loads are calculated independently based on their overall thermal conductances (UA). Thus, for a two-compartment refrigerator (freezer and fresh-food), the minimum values of power consumption required to keep each compartment at the desired temperatures are calculated from:

$$W_{ideal,fz} = \frac{UA_{fz}\left(T_{amb} - T_{fz}\right)}{COP_{ideal,fz}} \tag{3}$$

$$W_{ideal,ff} = \frac{UA_{ff}\left(T_{amb} - T_{ff}\right)}{COP_{ideal,ff}} \tag{4}$$

where

$$COP_{ideal,fz} = \frac{T_{fz}}{T_{amb} - T_{fz}} \tag{5}$$

$$COP_{ideal,ff} = \frac{T_{ff}}{T_{amb} - T_{ff}} \tag{6}$$

The overall power consumption is obtained adding Eqs. (3) and (4). Thus, the coefficient of performance of an ideal cycle, COP_{ideal}, is calculated from:

$$COP_{ideal} = \frac{UA_{fz}\left(T_{amb} - T_{fz}\right) + UA_{ff}\left(T_{amb} - T_{ff}\right)}{W_{ideal,fz} + W_{ideal,ff}} \tag{7}$$

and the average cabinet air temperature, T_{int}, can be obtained from Eq. (2).

Power consumption of a real cycle with an ideal compressor

The thermodynamic losses of a real refrigeration cycle can be classified into internal and external. The external irreversibilities are due to heat transfer with finite temperature differences, whereas the internal irreversibilities are associated with fluid friction in the cycle components and in the tubes connecting them. In order to account for the thermodynamic irreversibilities due to the cycle components but the compressor, the cycle efficiency was defined as follows:

$$\eta_{cycle} = \frac{W_{ideal}}{W_s} = \frac{COP_{cycle}}{COP_{ideal}} \tag{8}$$

where W_s is the isentropic compression power, calculated from

$$W_s = w\left(h_{2,s} - h_1\right) \tag{9}$$

where h_1 is the enthalpy at the compressor inlet [J/kg], $h_{2,s}$ is the enthalpy at the compressor outlet [J/kg] calculated assuming an isentropic compression from p_e to p_c, and w is the refrigerant mass flow rate [kg/s].

Overall compression efficiency

The overall compression efficiency, η_g, is defined as the ratio between the electrical power consumed by the compressor, W_{actual}, and the power consumed during an isentropic compression (see Eq. (9)):

$$\eta_g = \frac{W_s}{W_{actual}} = \frac{COP_{actual}}{COP_{cycle}} \tag{10}$$

Cycling efficiency

In addition to the sources of irreversibility already mentioned, cycling losses due to the on-off control pattern should also be accounted for. The cycling efficiency can be defined as the ratio between the cycle-averaged thermal load and the cycle-averaged cooling capacity:

$$\eta_{cycling} = \frac{\frac{1}{t_{on}+t_{off}}\int_0^{t_{on}+t_{off}} \left(UA_{fz}\Delta T_{fz} + UA_{ff}\Delta T_{ff} + W_{\text{int}}\right)dt}{\frac{1}{t_{on}+t_{off}}\int_0^{t_{on}+t_{off}} Q\,dt} \tag{11}$$

where W_{int} represents the rate of energy dissipation within the refrigerated compartments due to the evaporator fan, light bulb and electrical heaters, and $t_{on}+t_{off}$ is the cycling period.

System efficiency and overall energy consumption

The power consumed by the refrigerator as a whole is obtained adding the actual compression power to the power consumed by the other components, such as condenser and evaporator fans, control boards and light bulbs. Thus, the manipulation of Eqs. (1) to (11) yields to the following expression for the cycle-averaged overall power consumed by the refrigeration system, W_{system}:

$$W_{system} = \frac{\frac{1}{t_{on}+t_{off}}\int_0^{t_{on}+t_{off}} \left(UA_{fz}\Delta T_{fz} + UA_{ff}\Delta T_{ff} + W_{\text{int}}\right)dt}{COP_{ideal}\cdot\eta_{cycle}\cdot\eta_g\cdot\eta_{cycling}} + W_{other} \quad (12)$$

It is noteworthy that the equation above actually describes the refrigerator energy consumption as a function of three fundamental efficiencies and the coefficient of performance of an ideal cycle. The product of these parameters stands for the coefficient of performance of the refrigeration system, COP_{system}:

$$COP_{system} = COP_{ideal}\cdot\eta_{cycle}\cdot\eta_g\cdot\eta_{cycling} \quad (13)$$

As will be shown below, an analysis of each parameter in Eq. (13) not only allows the qualitative and quantitative comparisons between different refrigeration systems, but also points out the major sources of thermodynamic losses.

Experimental Work

Tests were carried out with a 450-liter top-mount frost-free refrigerator with two refrigerated compartments (freezer and fresh-food), whose temperatures are controlled independently. The fresh-food temperature is controlled by a thermal-mechanical damper that varies the air flow rate to this compartment, whereas the freezer compartment temperature is controlled by a thermostat that switches the compressor on and off. The evaporator is of the tube-fin type placed within the freezer compartment, whilst a forced air wire-and-tube condenser is located at the bottom part of the cabinet. HFC refrigerant 134a is used as the working fluid and ISO10 POE oil is employed for compressor lubrication. Figure 1 shows a schematic representation of the refrigerator under analysis. The refrigerator was instrumented with thermocouples, pressure transducers, and high resolution power meters, as summarized in Table 1.

Table 1. Summary of the measured parameters.

Symbol	Description
T_{ff}	Average fresh-food temperature
T_{fz}	Average freezer temperature
T_{int}	Average cabinet air temperature
T_{amb}	Average surrounding air temperature
T_1	Refrigerant temperature at the compressor suction
T_2	Refrigerant temperature at the compressor discharge
T_3	Refrigerant temperature at the capillary tube inlet
p_2	Discharge pressure
p_1	Suction pressure
w	Refrigerant mass flow rate
W_{system}	Overall power consumption
W_{actual}	Compressor power consumption
W_{int}	Evaporator fan power consumption

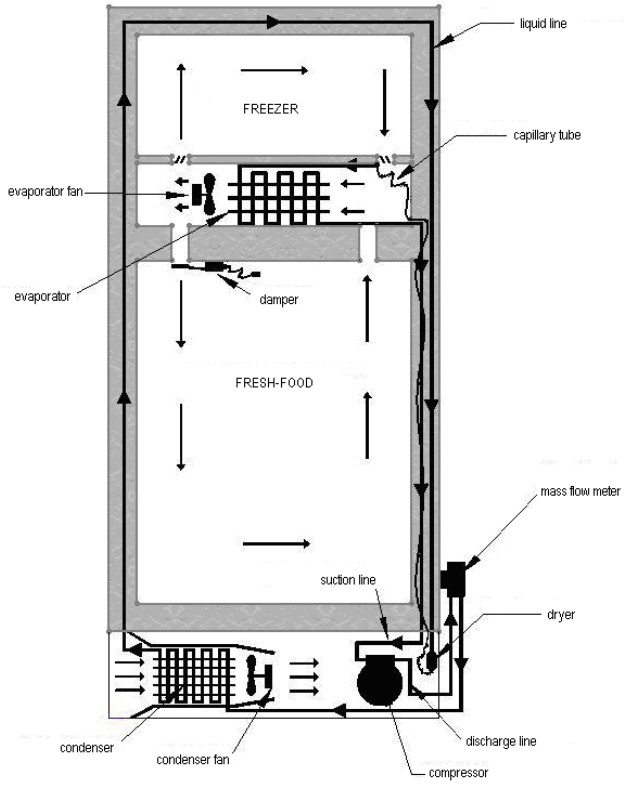

Figure 1. Schematic representation of the household refrigerator.

Temperature, pressure and power measurement

The cabinet air and refrigeration loop temperatures were measured using T-type thermocouples with a measurement uncertainty of ±0.2°C. The refrigerant temperatures were approximated by the temperatures measured at the surface of the pipe fittings, but employing a thin electrical insulation media between the thermocouple and the tube fittings in order to avoid undesired electrical biasing. For the compressor, the inlet and outlet temperatures were measured at positions located 100 mm far from the compressor shell in order to avoid thermal biasing. The thermocouples used for measuring the cabinet air temperatures were brazed in cylindrical-shape structures made of copper, according to the recommendation of the ISO/FDIS 15502 standard (2005). These masses act as thermal filters that reduce the high frequency, low amplitude temperature oscillations typical of the turbulent air flow.

The refrigerant pressures at the compressor suction and discharge ports were measured by strain gage absolute pressure transducers with a measurement uncertainty of ±1%. The transducers were installed at the same height of the pressure taps using small bore pipe fittings in order to avoid the influence of the fluid column. In addition, the supplied voltage signal was additionally monitored and controlled.

The power consumption of the compressor, evaporator fan and condenser fan, control board, light bulbs and defrost heaters was measured using a digital power analyzer with a measurement uncertainty of ±0.1%. The compression power was monitored during the refrigerator tests, whereas the power consumption of the other components was measured *a priori*, before testing the refrigerator. Oscillations of up to ±2% were observed in the voltage supplied to the compressor, which were incorporated into the propagated measurement uncertainty.

The methodology also requires the experimental determination of the refrigerant mass flow rate and the thermal conductances of the

refrigerated compartments. The procedures used to measure both of them are described below. It is worthy of note that the propagated uncertainties of the energy consumption, thermal loads, cooling capacity and *COP* never exceeded ±5%.

Refrigerant mass flow rate

The refrigerant mass flow rate is required for the computation of the instantaneous cooling capacity through the following energy balance in the control volume illustrated in Fig. 2:

$$Q = w(h_5 - h_4) \tag{14}$$

where h_4 and h_5 are the refrigerant enthalpies at the evaporator inlet and outlet ports. It should be noted that two-phase refrigerant flow is observed at points (4) and (5), which prevents the enthalpies from being calculated as a function of the measured pressure and temperature. To address this, an energy balance in the capillary tube-suction line heat exchanger is invoked, yielding h_5-h_4 = h_1-h_3, where h_1 and h_3 are the refrigerant enthalpies at the compressor inlet and condenser outlet ports, respectively. Thus, since there are subcooled liquid at point (3) and superheated vapor at point (1), the cooling capacity can be calculated based on the measurement of the suction and discharge pressures, the mass flow rate and the compressor inlet and condenser outlet temperatures.

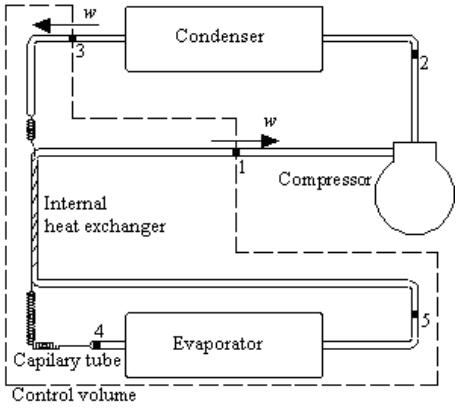

Figure 2. Control volume used in the cooling capacity calculation.

In this study, two different methods were investigated to determine the refrigerant mass flow rate: the direct measurement using a Coriolis-type mass flow meter insulated with a 20 mm thick layer of polystyrene foam and installed at the compressor discharge (see Fig. 1), and the indirect measurement through the compressor curves available from the manufacturer. The latter is based on the theory of reciprocating compressors (Gosney, 1982), according to which the refrigerant mass flow rate is calculated from:

$$w = \frac{\eta_v V N}{v_1} \tag{15}$$

where N is the compressor angular speed [Hz], V is the compressor stroke [m^3], v_1 is the specific volume at the compressor inlet, and η_v is the compressor volumetric efficiency, calculated from:

$$\eta_v = a + b\frac{p_c}{p_e} \tag{16}$$

where p_c and p_e are the condensing and evaporating pressures [Pa], and a and b are empirically fitted coefficients. Figure 3 shows a plot of the volumetric efficiency of the compressor used in the refrigerator under analysis as a function of the pressure ratio (p_c/p_e) obtained from experimental data: (i) supplied by the compressor manufacturer, (ii) acquired using a hot-gas calorimeter facility (ASHRAE S23, 1993), and (iii) acquired with the refrigerator instrumented with a Coriolis mass flow meter. Similar results were obtained with all three approaches, providing a single equation for the compressor volumetric efficiency, with a = 0.9434 and b = 0.02214.

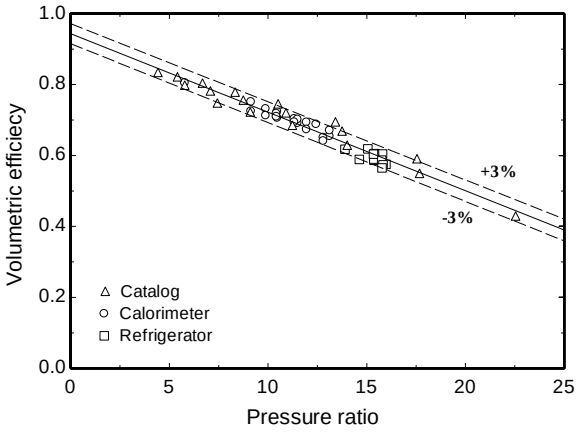

Figure 3. Correlation between the volumetric efficiency and pressure ratio.

Cabinet thermal conductances

The cabinet thermal loads are calculated based on the conductances of each refrigerated compartments, UA_{fz} and UA_{ff}. Basically, two methods can be tested to obtain the conductances: the so-called reverse heat leakage (Vineyard et al., 1998; Gonçalves et al., 2000) and the direct approach (Gonçalves, 2004). The first is called reverse as the indoor temperatures are kept higher than the surrounding temperature due to power dissipation within the refrigerated compartments through electric heaters. During the test, the refrigeration system is switched off, and the cabinet and surrounding temperatures and the power dissipated by the electric heaters (W_{fz}, W_{ff}) are monitored at the steady-state condition. The evaporator fan must be switched on (W_{int}) not only to homogenize the compartment temperatures (T_{fz}, T_{ff}), but also to provide the actual convection on the cabinet walls. The thermal conductances are then calculated from an energy balance, as follows:

$$UA_{fz}(T_{fz} - T_{amb}) + UA_{ff}(T_{ff} - T_{amb}) + S = 0 \tag{17}$$

where S = –(W_{fz}+W_{ff}+W_{int}) is the source term, in [W]. It is noteworthy that the results of at least two tests performed under different conditions are required. The conductance values are then obtained by the least squares method.

In the direct approach, the refrigeration system is kept running at steady-state regime so that the thermal loads are equal to the cooling capacity and, therefore, the thermal conductances can also be calculated from Eq. (17) with the source term defined as S = Q, where Q is the cooling capacity obtained from Eq. (14).

Figure 4 compares the results achieved using both methods, where positive values refer to the direct tests (i.e., heat entering the cabinet, $S > 0$) and the negative values to the reverse tests (i.e., heat being transferred to the surrounding air, $S < 0$). As can be seen, both methods provide similar values for the cabinet conductances, UA_{fz} = 0.88 W/K and UA_{ff} = 1.21 W/K, fitted to the

experimental data within a ±10% error band. The raw data obtained from the direct and reverse tests are summarized in Table 2, where *S* is the source term of Eq. (17).

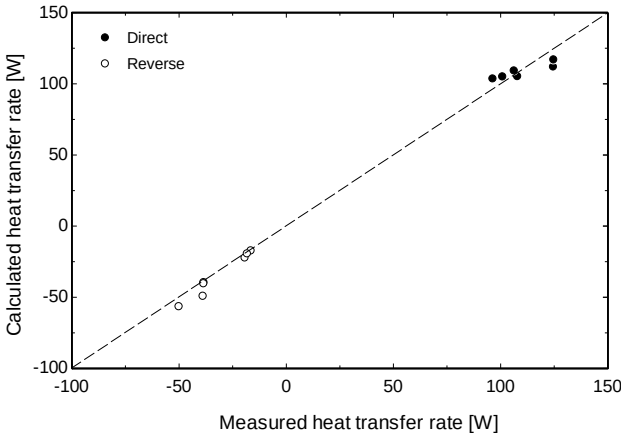

Figure 4. Comparison between the measured and calculated cabinet thermal loads.

Table 2. Experimental data used for thermal load calculations.

Method	Test No.	*S*, W	T_{amb}, °C	T_{fz}, °C	T_{ff}, °C
Direct	1	124.6	43.1	-23.0	1.6
	2	107.8	32.1	-28.7	-7.3
	3	100.9	25.0	-31.4	-15.8
	4	124.7	43.0	-22.3	-1.6
	5	106.3	32.0	-28.4	-9.8
	6	96.3	25.1	-31.9	-14.6
Reverse	7	-50.0	25.3	54.1	47.7
	8	-38.9	23.2	47.7	42.9
	9	-19.3	25.1	36.3	34.0
	10	-38.5	25.2	52.5	38.5
	11	-16.5	25.2	36.5	31.2
	12	-38.6	25.1	52.4	38.9
	13	-18.2	25.2	37.9	31.9

Results

The experiments were carried out for three different ambient temperatures: 25, 32 and 43ºC. A nominal refrigerant charge of 138 g was employed, and the damper and thermostat were adjusted to the maximum cooling position. During the tests, the refrigerator was kept running according to a cycling pattern. The experimental data were processed considering three cycles in a row. Table 3 summarizes the results of the experiments in terms of the average Carnot and system *COP*, energy consumption and runtime ratio (i.e., the ratio between the compressor runtime and the whole on-off cycle period). As expected, both Carnot and system *COP* drop with the rising ambient temperature as the temperature difference between the thermal reservoirs increases (see Fig. 5). Furthermore, it is worth noting that in Fig. 5 the refrigeration efficiency, defined as the ratio between the Carnot and system *COP*, is fairly constant with values around 20%.

Table 3. Summary of the experimental results.

Ambient temperature, °C	25.2	31.8	43.1
COP_{ideal}	8.2	7.1	5.6
COP_{system}	1.7	1.5	1.2
Runtime ratio	0.35	0.46	0.68
Energy consumption, kWh/month	27.9	38.4	58.4

Figure 6 shows that the runtime ratio increases with the rising ambient temperature, as does the overall energy consumption, which is a consequence of the thermal load augmentation.

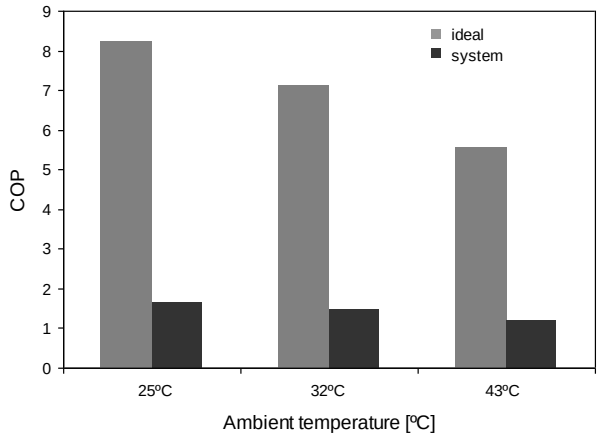

Figure 5. Variation of the measured coefficient of performance with ambient temperature.

The results obtained for the average cycling, compression and cycle efficiencies are presented in Fig. 7. As can be seen, the compression efficiency increases with the ambient temperature because of a reduction in the pressure ratio, which also causes an increase in the overall refrigeration efficiency. In all cases, it was noted that the cycle efficiency is responsible for the major part of the thermodynamic losses, suggesting that the heat exchangers (condenser and evaporator) have a great potential for improvement. The cycling losses, on the other hand, showed to be of no practical significance, which is probably due to the low amount of refrigerant employed in small-capacity household refrigerators.

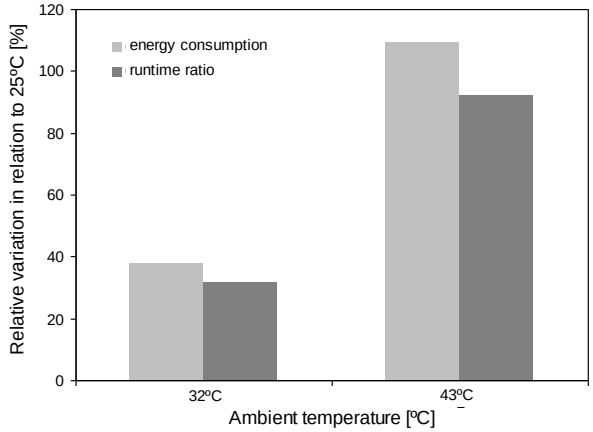

Figure 6. Variation of the energy consumption and runtime ratio with ambient temperature in comparison to an ambient temperature of 25ºC.

Figures 8 to 10 show the instantaneous values of the power consumption, heat transfer rates and system efficiencies for an ambient temperature of 32ºC. Figure 8 depicts the instantaneous power consumption of an ideal (Carnot) cycle, of a real cycle with an ideal compressor, of a real cycle, and the overall power consumption of the refrigerator, which also accounts for the evaporator and condenser fans. Again, it can be seen that the cycle losses increase the power consumption by 150% in comparison to the Carnot cycle in the case where an ideal compressor is used. If a real compressor is used, the power consumption increases by 300%.

As expected, the energy consumption of the evaporator and condenser fans has a minor influence upon the overall energy consumption.

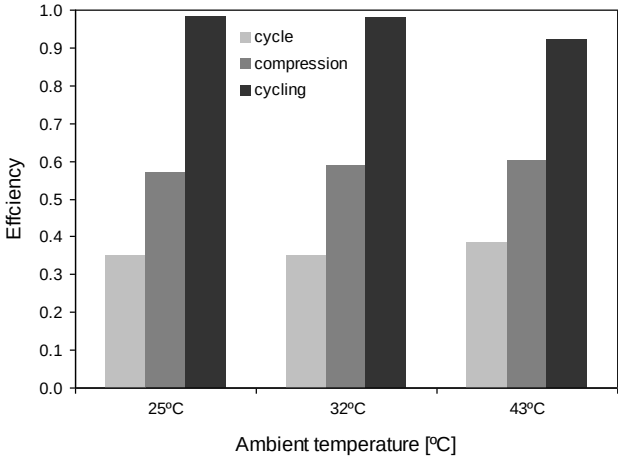

Figure 7. Variation of the average efficiencies with ambient temperature.

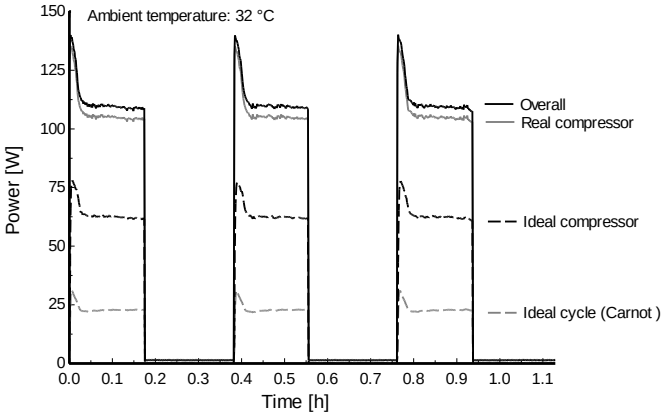

Figure 8. Variation of the power consumption with time.

Figure 9 presents the instantaneous values (solid lines) calculated for both the cooling capacity and the thermal loads. During the system startup, the cooling capacity reaches a peak due to the large temperature difference between the evaporator coil and the cabinet air, which decreases slightly until the cut-off temperature is reached. The thermal loads, on the other hand, increase monotonically inasmuch the cabinet air temperature decreases and the temperature difference between the indoor and outdoor environments increases. During the off period, the cooling capacity is very small, while the thermal load is reduced as the cabinet air temperature increases. In addition, the dotted lines represent the average values calculated for both the cooling capacity and the thermal load. The small difference between them shows that the cycling losses have a small contribution to the system inefficiency.

Figure 10 depicts the instantaneous contributions of each component of the refrigeration efficiency. It can be noted that the cycling efficiency has a constant value since it is obtained through a cycle-averaged calculation. The compression and cycle efficiencies remain practically constant during the refrigerator operation. Of course, these efficiencies have no significance during the off period. Again, the low cycle efficiency seems to be responsible for the major part of the refrigerator losses, whilst the cycling efficiency is close to unity.

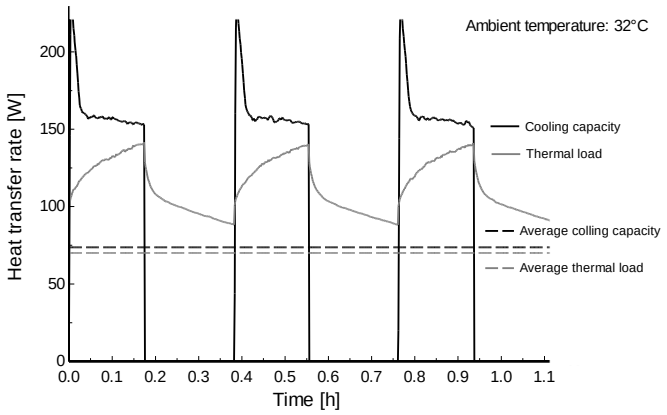

Figure 9. Variation of the cooling capacity and thermal load with time.

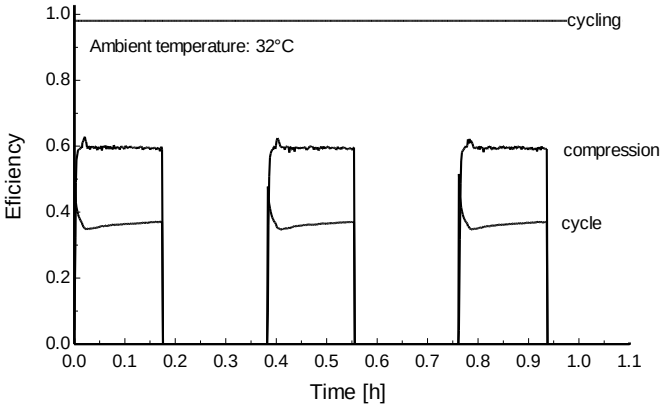

Figure 10. Variation of the system efficiencies with time.

Concluding Remarks

A novel methodology for analyzing experimental refrigerator data was introduced in this study. The methodology maps the thermodynamic losses of the refrigeration system in terms of the following efficiencies: (i) Carnot coefficient of performance, (ii) efficiency of a real cycle operating with an ideal compressor, (iii) compression efficiency of a real compressor, and (iv) cycling efficiency. The methodology proposed herein points out the thermodynamic losses of the refrigeration cycle, identifying opportunities for energy performance enhancement. In addition, the methodology enables the comparison of different refrigerators at the same thermodynamic baseline.

The tests were carried out with a 450-liter top-mount frost-free refrigerator. Results have shown that the cycle efficiency is responsible for the major part of the refrigerator losses, whilst the cycling efficiency is close to unity. An overall refrigeration efficiency of 21% was observed, suggesting that there is a broad margin for improvements. Albeit the methodology was originally developed for household refrigerators, it can be easily extended to any kind of vapor compression refrigeration systems.

Acknowledgements

This study was carried out at the POLO Laboratories under National Grant No. 573581/2008-8 (National Institute of Science and Technology in Cooling and Thermophysics) funded by the CNPq agency. Thanks are also addressed to Messrs. M. Waltrich and F.T. Knabben for their valuable support with the experiments.

References

ANSI/AHAM HRF-1, 2004, "Energy performance and capacity of household refrigerators, refrigerator-freezers and freezers", American National Standards Institute, Washington DC, USA.

ASHRAE S23, 1993, "Methods of testing rating positive displacement refrigerant compressor and condensing units", American Society of Heating, Refrigerating and Air Conditioning Engineers, Atlanta GA, USA.

Bansal, P.K., 2003, "Developing new test procedures for domestic refrigerators: harmonisation issues and future R&D needs – a review", *International Journal of Refrigeration*, 26, pp. 735-748.

Gonçalves, J.M., 2004, "A steady-state semi-empirical simulation model for frost-free refrigerators" (in Portuguese), DEng thesis, Department of Mechanical Engineering, Federal University of Santa Catarina, Florianópolis SC, Brazil, 181 p.

Gonçalves, J.M., Melo, C., Vieira, L.A.T., 2000, "Experimental study of 'frost-free' refrigerators, Part I: Heat transfer through the cabinet walls" (in Portuguese), Proceedings of the 1st National Congress of Mechanical Engineering, Natal, RN, Brazil.

Gosney, W.B., 1982, "Principles of refrigeration", Cambridge University Press, Cambridge, UK.

Hermes, C.J.L., Melo, C., Lacerda, V.T., 2004, "A new approach to analyze the start-up and cycling transients of 'no-frost' refrigerators based on standardized test data" (in Portuguese), Proceedings of the 3rd National Congress of Mechanical Engineering, Belém, PA, Brazil.

ISO/FDIS 15502, 2005, "Household refrigerating appliances – characteristics and test methods", International Organization for Standardization, Geneva, Switzerland.

Vineyard, E.A., Therese, K.S., Kenneth, E.W., Kenneth, W.C., 1998, "Superinsulation in refrigerators and freezers", *ASHRAE Transactions*, 104 (2), pp. 1126-1134.